Functional Surfactants for Carbon Nanotubes: Effects of Design

Friederike Ernst,*,† Timm Heek,‡ Antonio Setaro,† Rainer Haag,‡ and Stephanie Reich†

Freie Universität Berlin, Department of Physics, and Freie Universität Berlin, Department of Chemistry and Biochemistry

E-mail: f.ernst@fu-berlin.de

Phone: +49 (0)30 83856156. Fax: +49 (0)30 83856081

Abstract

Surfactants are needed to create stable suspensions of carbon nanotubes. Increasingly, these surfactants are given additional functionalities, resulting in bigger and more complex molecules with several subunits. We investigate the effects of the assembly of these subunits on both the molecule's performance as a surfactant and the interaction between the functional core and the nanotube by energy transfer. This results in a best practice guide for designing functional surfactants with π - π stacking cores, and affords more general insights which are applicable to non π - π stacking systems as well.

Introduction

Single walled carbon nanotubes (SWNTs) are hollow cylinders with walls one atomic layer of carbon thick; their diameters typically range between 0.5 nm and 2 nm, while their length can

*To whom correspondence should be addressed

†Department of Physics of the Freie Universität Berlin, Arnimallee 14, 14195 Berlin

‡Department of Chemistry and Biochemistry of the Freie Universität Berlin, Takustraße 3, 14195 Berlin

reach centimeters. The nanoscale across the tube axis causes the tubes to display quantum phenomena stemming from strong quantization of electronic states and delocalization.[1,2] Unlike other nanoscale systems, these properties are easily accessible on the macroscopic scale owing to the length of the nanotube. However, these optoelectronic phenomena only manifest themselves in sufficiently isolated pristine tubes; typically, nanotubes occur in bundles and need to be separated from each other first.[3]

Solubilization of pristine carbon nanotubes in solutions requires additional surfactants which broadly fall into three classes: biomolecules, polymers, and small molecules.[4] Huge advances have been made with all three groups in the last ten years. Small molecules were the first surfactants used, and still encompass most standard surfactants such as sodium cholate (SC) or sodium dodecylbenzene sulfonate (SDBS).[5–7] Their main advantage is that they are cheap, easy to come by, and simple to use. These small molecules have a hydrophobic tail and and a hydrophilic headgroup and suspend nanotubes by shielding them from the aqueous environment, either in a micellar structure or by stacking on the tube.[8] Polymers and biomolecules can come with additional functionalities: Polymers have proved very useful in the incorporation of nanotubes into organic photovoltaic devices.[9–11] Nanotubes are wrapped in a chromophore containing polymer, and the chromophore forms heterojunctions with the nanotube, allowing energy or charge to be transferred into the nanotube upon irradiation. Aromatic polymers have also been shown to solubilize nanotubes with a high chiral selectivity.[12,13] Efforts with biomolecules mostly aim at increasing the chiral selectivity of the surfactants and integrating them into biological systems.[14–16]

Recently, we adapted small molecules such that they not only serve as surfactants, but also incorporate an additional functionality.[17] Energy transfer complexes of nanotubes and chromophores are of considerable interest and have been studied previously, both in polymer-nanotube complexes and in complexes created by micelle swelling.[18–20] In the micelle swelling technique nanotubes are suspended by standard surfactants in water, into which dye molecules solved in organic media are stirred. The organic solvent evaporates, while the dye enters the micelle and π -π stacks on the nanotube.[21] We incorporated this energy transfer functionality directly into a surfactant.[17] Several

other functionalities are conceivable, for instance, the incorporation of molecular switches.[22] However, adding more functional parts to the surfactant also introduces additional degrees of freedom. How are these molecules best assembled?

In this paper, we systematically vary the different building blocks of the functional surfactant. While we keep the functional core unchanged, the parts of the functional surfactant responsible for water-solubility and debundling of the nanotubes are altered. These modifications not only substantially alter the molecules suitability as a surfactant but also impinge on the mechanism of the energy transfer. We relate the changes in behavior to the morphological features. We expect that the guidelines we develop for the successful design of complex functional perylene-based molecules are directly applicable to other systems that rely on the π - π stacking interaction. Additionally, many aspects may also be relevant for functional surfactants based on different exchange interactions.

Results and Discussion

We previously introduced a novel surfactant which was rationally designed such that it solubilizes nanotubes efficiently in aqueous solution independently of pH and forms ultra efficient energy transfer complexes with the nanotubes through a $\pi - \pi$ stacking mechanism.[17] The surfactant we introduced, see Figure 1, **A**, consists of three functional units: The aromatic core (red) is a perylene derivative dye which is responsible for the energy transfer complexes formed with the tubes, discussed in detail elsewhere.[17] The dye was combined with a polyglycerol dendron (blue) to ensure water solubility[23] and enhance biocompatibility.[24] The third part is constituted by two hydrophobic alkyl chains comprising 16 carbons each (green). These alkyl chains are relevant for the individualization of the nanotubes.

A is part of an extensive family of molecules and we would now like to systematically elucidate the effects of the variation of the individual components of the surfactant. All ten examined molecules are pictured in Figure 1. The perylene core was left untouched while the alkyl

chains and the dendrons as well as their linkers were changed. In the wake of these alterations, the molecules abilities to suspend nanotubes in water and individualize them efficiently changes starkly. The molecules also display varying capabilities of forming excitation-transfer complexes with the nanotube.

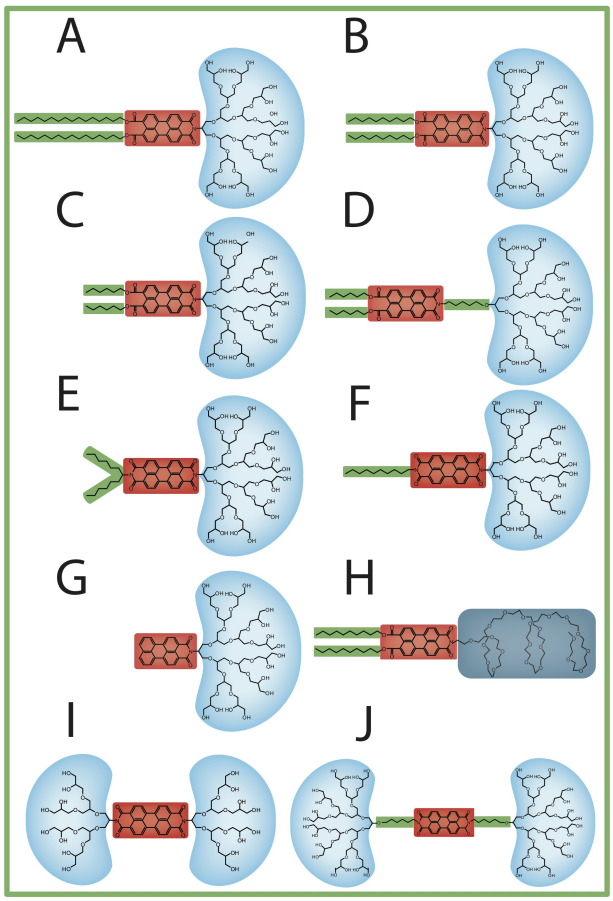

Figure 1: Chemical structures of the surveyed perylene derived surfactant molecules. Perylene cores are color coded in red, alkyl chains in green, polyglycerol dendrons in light blue. **H** features a PEG chain (dark blue) instead of a dendron.

The molecules performance as a surfactant was quantified with a combination of absorbance and photoluminescence (PL) measurements. Absorbance measurements allow us to infer the amount of nanotubes suspended in the sample; typical absorption features seen for SWNTs are the S_{11} transitions between 950 nm and 1350 nm and the S_{22} transitions between 620 nm and 830 nm.[1] While all tubes contribute to absorption, only sufficiently individualized semiconducting nanotubes display photoluminescence. Optical deexcitation is a comparatively slow process and is only

observed when non-optical pathways, i. e., recombination in co-bundled metallic tubes, are not available.[1]

To ensure comparability, all samples were prepared with the same protocol, cf. Experimental Section. In Figure 2 a we show the suspension and individualization behavior of our surfactants. The X-axis quantifies the number of bundles in the sample, while the Y-axis indicates the PL intensity per tube. The photoluminescence per nanotube was calculated as the ratio of the sum of the (7,5) and (7,6) PL intensities divided by the absorbance peak at 650 nm.[a] The number of bundles is given by the ratio of the absorbance background and the absorbance peak at 650 nm: large bundles scatter light extensively, resulting in increased optical extinction.[25] The absorbance background was evaluated at 950 nm, the plateau between S_{11} and S_{22} peaks. The raw absorbance data of all samples is supplied in the Supporting Information, Figure 7.

From Figure 2 a it is apparent that molecules **A**, **B**, and **D** are very good surfactants. They suspend large numbers of individual nanotubes and few bundles. All other molecules suspend nanotubes mainly in bundles in varying quantities. While the monochained compound **F** suspends no tubes at all, compound **J** suspends large numbers of bundles which are small enough to remain suspended during centrifugation, cf. Experimental Section. This difference in debundling efficiency is explained by the hydrophilic-lipophilic balance of the individual molecules.[26] In Figure 2 b we show the same PL intensity on the Y-axis, but this time plotted against the total length of the alkyl chains in the compound. The trend is clear: the debundling efficiency increases with increasing alkyl chain component up to a total length of 20-C, compound **B**. Compound **A** has two C-16 chains, and its debundling efficiency is lower than that of **B**. The potential energy of the nanotube-surfactant complex comprises two main terms. Firstly the energy gained from the π orbital overlap between nanotube sidewall and perylene, and secondly the energy expended by the surfactant for not forming a micelle and thereby shielding the hydrophobic alkyl chains from the water. In the limiting case of very long alkyl chains the hydrophobicity is increased such that

[a]The S_{22} transitions of (7,5) and (7,6) tubes are the main contributers to the absorbance at 650 nm. It should be noted that both S_{11} and S_{22} absorption contribute to photoluminescence. However, S_{11} and S_{22} absorption are proportional for all samples, see Supporting Information, Figure 7.

the surfactant is expected to form micelles. We surmise that this is already starting to happen for compound **A**. A part of the molecules is not available for suspending nanotube via adsorption of the perylene core onto the tube wall; thus **A**'s efficiency as a surfactant is lower than **B**'s.

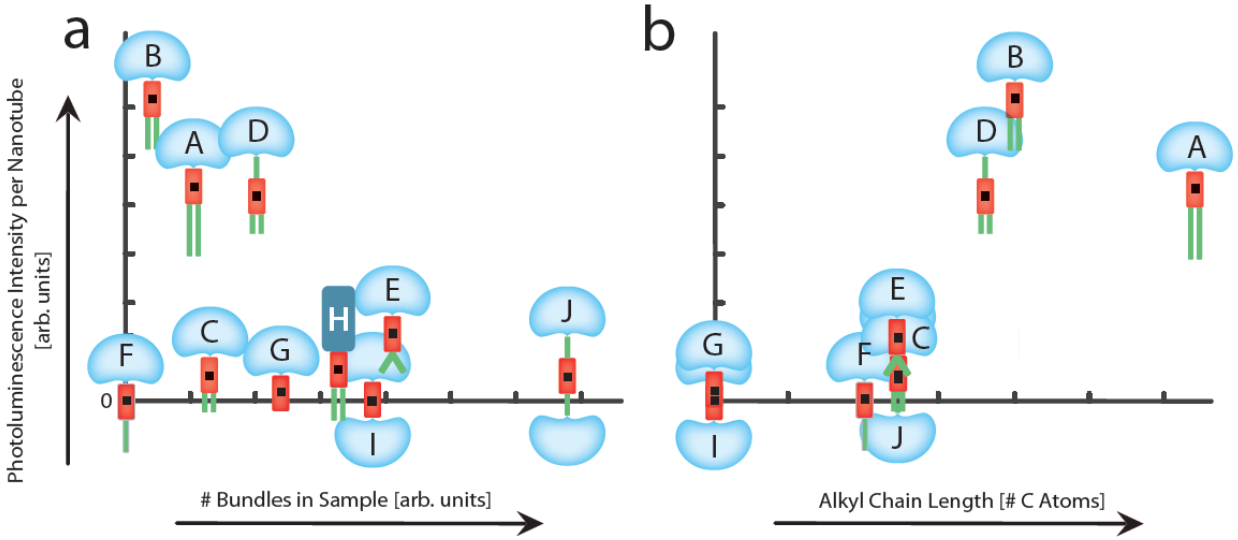

Figure 2: Solubilization and individualization capabilities of molecules **A** - **H**. **a)** The number of bundles in the samples against the PL intensity per tube. **b)** Total alkyl chain length of the molecule against PL intensity per tube. For explanation of the detailed quantities, see text.

Backes et al. surveyed perylene bisimide based surfactants with pH sensitive Newkome dendrons previously.[27] Three of the molecules covered in this study have direct equivalents in our work: **E**, **F**, and **J**. All three of these molecules perform poorly in our study, whereas Backes et al. find them to individualize nanotubes better than SDBS. We assess the degree of individualization through the optical properties of the suspended nanotubes, while Backes et al. do so through AFM measurements and the changes in the absorption spectrum of perylene which they use as an indicator of the stacking states. We attribute this discrepancy between our results and theirs to the Newkome dendrons present in Backes compounds, which may wrap around the nanotube electron depleted by the perylene core.[27] Our charge-neutral dendron has no affinity toward the nanotube and extends into the surrounding water.

In addition to varying in their qualities as a surfactant, the ten molecules also vary in their interaction mechanism with the nanotubes. Seven of the investigated compounds result in samples with nanotube photoluminescence, but only six also display energy transfer. Two compounds

suspend nanotubes in bundles, while one fails to interact with the nanotubes completely.

In the remainder of the paper we will discuss the properties of all compounds individually in detail and attribute them to the molecules morphological features.

A, **B**, and **C** differ from each other only in the length of their two parallel alkyl chains, containing 16, 10, and 6 carbon atoms, respectively. **A** and **B** both solubilize nanotubes in water, and their perylene core π - π stacks on the tube, allowing energy transfer complexes to form. A PLE map of **B** solubilized tubes is given in Figure 3 a. The peaks above the grey line stem from the direct excitation of the indicated chiralities, while the peaks below the grey line are attributed to the indirect excitation through the adsorbed perylene. Free perylene-imido-diesters have an absorbance of 420 nm - 550 nm and an emission 520 nm - 700 nm. When $\pi - \pi$ stacked on the nanotube, however, the characteristic emission is quenched, the excitation is passed into the nanotube, and a subsequent emission at the E_{11} energy of the nanotube is seen. These are the peaks below the grey line in Figure 3 a. The underlying energy transfer process is discussed in detail elsewhere.[17]

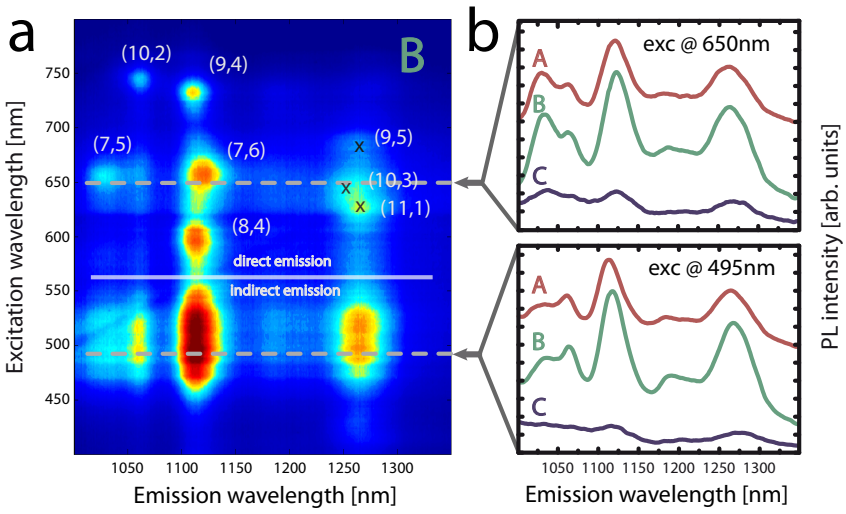

Figure 3: **a)** Photoluminescence map of nanotubes solubilized with **B**. A line separates the peaks which stem from the direct excitation of the individual chiralities above 560 nm from the emission of the tubes after indirect excitation through the adsorbed perylene below 560 nm. **b)** PL lines of nanotubes solubilized with **A**, **B**, and **C** excited at 650 nm (top) and 495 nm (bottom).

Single line photoluminescence measurements of compounds **A**, **B**, and **C**, Figure 3 b, show the

differences between the compounds at excitation wavelengths of 650 nm (top), corresponding to the direct excitation of the E_{22} state of several chiralities, and 495 nm (bottom), the excitation of all chiralities through the adsorbed perylene. The emission from the indirect excitation through the perylene at 495 nm is directly proportional to the emission from the direct excitation for all compounds. Compound **B** with the 10-carbon chains individualizes nanotubes the most efficiently, followed closely by **A** with the longer 16-C chains. Compound **C** with the short 6-C chains does not individualize nanotubes efficiently, only trace luminescence was observed.

The lack of nanotube individualization through the shorter chained **C** could be explained by either the interaction mechanism between the two parallel alkyl chains and the nanotube, which might require a minimum length longer than 6-C, or by the reduced lipophilicity of the molecule. This question was evaluated with surfactant **D**. **D** differs from **C** in that it has an additional spacer alkyl chain between perylene core and dendron, placing it in overall alkyl chain length just below **B**, while retaining the short parallel alkyl chains of **C**. PL measurements show that nanotubes functionalized with **D** are individualized efficiently and energy transfer complexes are formed, comparably so to the best compound, **B**. A PLE map is supplied in the Supporting Information, Figure 8.

These measurements show that it is not the length of the terminal alkyl chains alone that determines the individualization efficiency. To evaluate whether the alkyl chains are needed at all, we investigated compound **G**. **G** suspends nanotubes in water as demonstrated in absorbance measurements, see Figure 4. The left panel shows absorbance measurements for several NT preparation concentrations at a fixed surfactant molarity, see Experimental Section. The solubilization process is analogous to the one previously shown for compound **A**.[17] The emission from the free perylene at 500 nm is quenched with the incremental addition of nanotubes. This is attributed to the larger number of π - π stacked perylene surfactant molecules: the number of surfactant molecules remains constant, while the number of available stacking sites increases. At the same time the nanotube absorption rises up to 0.09 g/l and falls hereafter. The quantity of suspended nanotubes decreases despite rising preparation concentrations after 0.09 g/l because there is not enough sur-

factant to sufficiently debundle the present tubes to save them from being centrifuged out in the preparation process.[17] Unlike the compounds with alkyl chains, however, the resulting solutions do not display any photoluminescence, indicating that **G** debundles nanotubes enough to keep them in the supernatant during the centrifugation in the sample preparation process, see Experimental Section, but does not individualize them. We conclude that the alkyl chains are not necessary for suspension, but crucial for individualization.

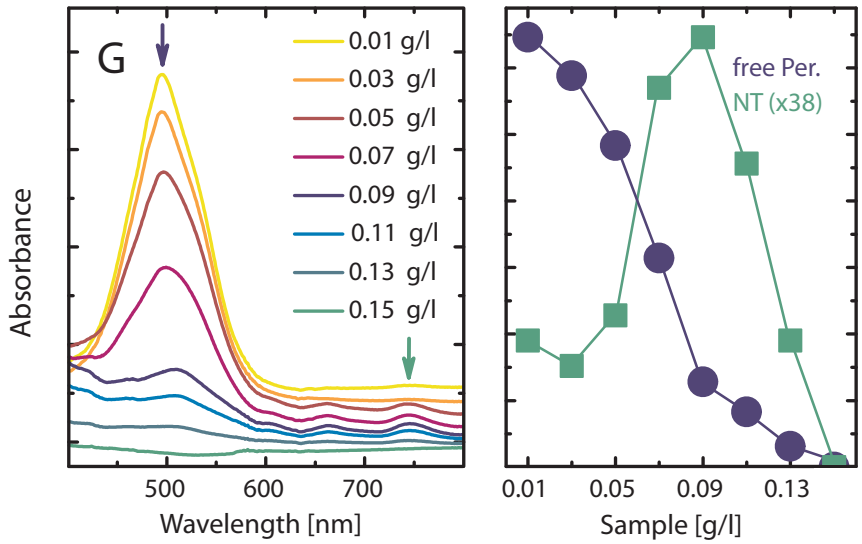

Figure 4: Absorbance measurements for samples prepared with **G** as a surfactant at a fixed molarity and varying amounts of nanotubes, given in g/l. Left: traces are offset for clarity. Right: absorption by the perylene core (blue circles), evaluated at 490 nm, and nanotube absorption (green squares), evaluated at 745 nm. The nanotube absorption is scaled by a factor of 38 for clarity.

The compounds with alkyl chains presented so far all feature two parallel alkyl chains. Are other types of morphology equally viable? Compound **E** has two C-6 alkyl chains that attach to the same carbon atom at an angle, forming a swallow tail. **E** suspends nanotubes very well. However, little photoluminescence is observed in these samples, cf. Figure 2. **E** is similarly inefficient at individualizing nanotubes as **C**, which has the same overall alkyl chain length. Just as in compound **C**, this does not affect the π - π stacking between nanotube and absorband: energy transfer is observed as demonstrated in photoluminescence measurements, cf. Supporting Information, Figure 9.

Compound **F** possesses a single C-10 chain. As seen in Figure 2, this surfactant does not suspends nanotubes at all. While all other compounds at least suspend nanotubes in bundles, the monochain actively impedes the interaction mechanism between perylene core and nanotube. This becomes apparent when comparing the solubilization through the monochain compound **F** to compound **G**, which has no chain. As discussed earlier, **G** stacks on the nanotube, it just lacks the ability to individualize the tubes. Why **F** fails to interact with the nanotubes completely is not clear at this point.

So far, we showed that the alkyl chains are needed for the individualization of the nanotubes by comparing the chained compounds to the naked perylene in compound **G**. But could the chains be replaced with a different structure all together? To probe this question we investigated compounds **I** and **J**, neither of which possesses free alkyl chains. Instead, they have a second dendron. For compound **I** the dendrons are of the smaller generation 2 and are directly attached to the perylene core via an imide bond. We chose the smaller dendritic structures because the generation 3 dendrons are structurally so bulky that they prevent any interaction of the perylene unit with the nanotubes. **J** has the larger generation 3 dendrons which are removed from the perylene unit with two C-6 alkyl spacer chains. Compound **I** completely fails to interact with the nanotubes, in all likelihood owing to steric hindrance by the dendrons. **J** solubilizes nanotubes efficiently, cf. Figure 2, and individualizes them to such an extent that photoluminescence can be observed, see Figure 5. The dark blue trace was recorded upon excitation at 650 nm. The light blue trace was recorded with an excitation of 495 nm, where the indirect emission via the excitation transfer would be expected. However, the signal is significantly smaller than for all other molecule-nanotube complexes which exhibit energy transfer, cf. Figure 3, and is compatible with a presence of non-resonant processes only.[1] This observation is further corroborated by the finding that no peaks are present between 1000 and 1100 nm, where the non-resonant processes are typically weak, and energy transfer peaks are present for the other compounds, cf. Figure 3. Moreover, the temporal stability of the solution prepared with compound **J** is poor. NTs solubilized with **J** rebundle on a time scale of days, see the inset of Figure 5. Solutions made with surfactants **A**, **B**, and **D** are stable over many months. This

differing temporal behavior may also reflect the fact that the mechanisms of interaction between molecule and nanotube is not the same for **J** on the one hand and for all the other compounds on the other hand.

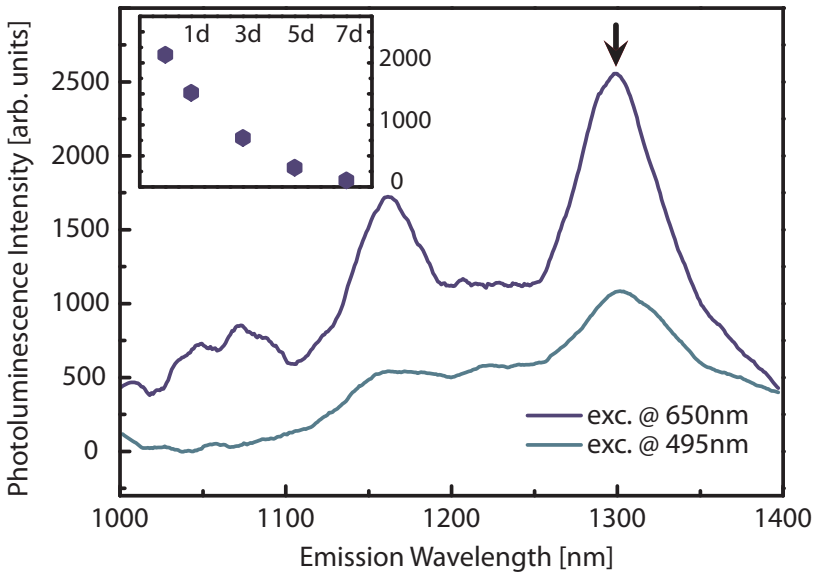

Figure 5: Photoluminescence measurements of nanotubes solubilized with compound **J** excited at 650 nm (dark blue) and 495 nm (light blue). Inset: temporal stability of the solution, data points give peak intensity at 1300 nm as a function of time since preparation.

Two things lead us to conclude that there is no π stacking between the nanotube and **J**: The degree of individualization afforded to the nanotubes by compound **J** is sufficient for photoluminescence, yet no energy transfer takes place. Additionally, the fast rebundling behavior is inconsistent with the high temporal stability observed for compounds **A**, **B**, and **D**. Given the spatial proximity required for electron orbital overlap in conjunction with the bulkyness of the two dendrons of compound **J**, this is not altogether surprising.

The final characteristic we investigated was the polyglycerol dendron. Compound **H** is equivalent to the optimal surfactant **B**, with two parallel 10-C alkyl chains, but instead of the polyglycerol dendron it possesses a linear PEG chain. **H** solubilizes and individualizes nanotubes and forms energy transfer complexes, see Figure 6. However, the solutions are far inferior to the ones made with **B** in luminescence intensity, cf. Figure 3 a. We thus conclude that it is preferable to choose a bulky dendron over a linear PEG chain for the hydrophilic part of the surfactant molecule.

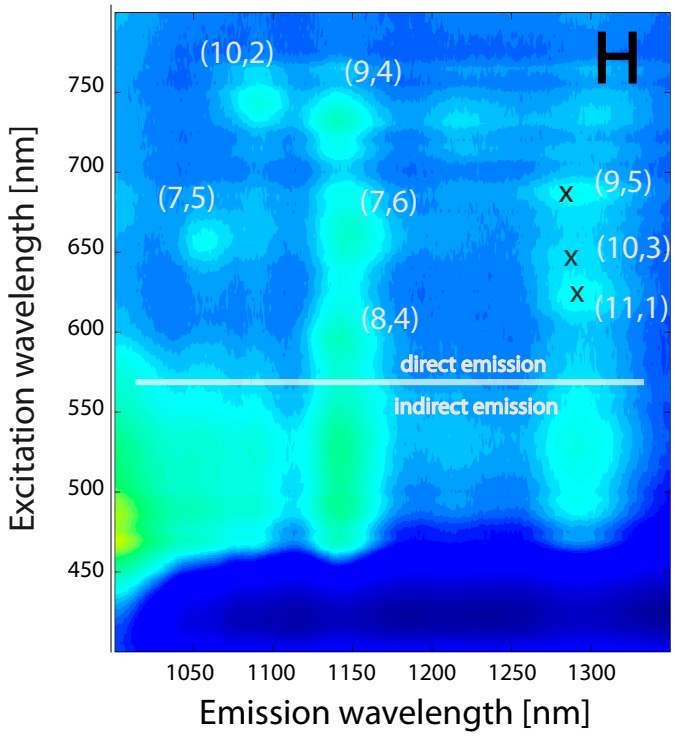

Figure 6: HiPco nanotubes solubilized with compound **H** which possesses a linear PEG chain instead of a dendron.

Conclusion

When designing a complex surfactant one faces the task of creating a single molecule with several functional units. The entire molecule needs to be water-borne and capable of suspending nanotubes. It also needs to be able to debundle nanotubes and keep them individualized over longer periods of time, while at the same time serving the additional functionality. This makes functional surfactants not only more complex in their design, but it makes the design more arbitrary: operational units need to be assembled and linked up, which can lead to many degrees of freedom. We have encompassed to survey a family of perylene based molecules. In this family the perylene unit is the added functionality: it can form energy transfer complexes with the nanotube via π - π stacking. However, we believe that many of our findings are applicable to a broad range of systems

and can be transferred to surfactant molecules with other functionalities.

Several aspects should be considered in the design of functional surfactants. For the hydrophilic part a polyglycerol dendron is far superior to a linear PEG chain. Mere suspension can be attained with compounds with two dendrons, but for efficient debundling and temporal stability of the resulting solutions, the molecule needs to incorporate alkyl chains. Where exactly these alkyl chains are located with respect to the functional core is inconsequential. We find a total length of 20-C to be optimal; longer alkyl chains entail a greater affinity for forming micelles, whereby the functional unit is removed from the nanotube.

As a starting point for the design of future functional surfactants whose function hinges on close proximity between functional core and nanotube we recommend a scheme with a polygylcerol dendron, the core and two parallel alkyl chains of 10-C length, each.

Experimental Section

The characterization of compounds **A**, **B**, and **I** has been published previously.[17,28,29] The synthesis and characterization of compounds **C** – **H**, and **J** is supplied in the Supporting Information online.

All samples were prepared at a fixed surfactant molarity of $6 \cdot 10^{-5}$M in deionized water without co-surfactant and with 0.1 g/l nanotubes. Additionally eight samples with compound **G** were prepared for which the SWNT preparation concentrations were varied between 0.01 g/l and 0.15 g/l. Samples were tip sonicated for 90 min and subsequently centrifuged at 30000 g and 23°C for 90 min. Hereafter, only the supernatant was kept. We used super purified HiPco SWNTs produced by Unidym^{TM} (batch SP0295) for the preparation of all samples.

PLE measurements were conducted in a Horiba Nanolog system. This system features a HgXe short arc lamp, from which a single excitation line is selected using a monochromator with two mechanically coupled gratings. The PL signals were recored with a nitrogen-cooled InGaAs detector (infrared) and a photomultiplier (vis).

Absorption measurements were taken in a Cary 5000 UV-vis-NIR spectrophotometer at room

temperature.

Acknowledgement

We gratefully acknowledge the financial support of the European Research Commission (grant number 210642) and the German Research Foundation (DFG via SFB 658, subprojects A6 and B7), and thank Dr. Ute Resch-Genger and Dr. Jutta Pauli at the Bundesanstalt für Materialforschung und -prüfung, Berlin, for access to the Cary 5000 UV-vis-NIR spectrophotometer. We further thank Emanuel Fleige for the preparation of mPEG-amine, and Sebastian Heeg and Pascal Blümmel for productive discussions.

References

(1) Reich, S.; Thomsen, C.; Maultzsch, J. *Carbon Nanotubes*; WILEY-VCH, 2004.

(2) Jorio, A.; Dresselhaus, M. S.; Dresselhaus, G. *Carbon Nanotubes - Advanced Topics in the Synthesis, Structure, Properties and Applications*; Springer, 2008.

(3) Reich, S.; Thomsen, C.; Ordejón, P. *Physical Review B* **2002**, *65*, 1–11.

(4) Zhao, Y.-L.; Stoddard, J. F. *Accounts of Chemical Research* **2009**, *42*, 1161–1171.

(5) Liu, J. *Science* **1998**, *280*, 1253–1256.

(6) Islam, M. F.; Rojas, E.; Bergey, D. M.; Johnson, a. T.; Yodh, a. G. *Nano Letters* **2003**, *3*, 269–273.

(7) Matarredona, O.; Rhoads, H.; Li, Z.; Harwell, J. H.; Balzano, L.; Resasco, D. E. *The Journal of Physical Chemistry B* **2003**, *107*, 13357–13367.

(8) Vaisman, L.; Wagner, H. D.; Marom, G. *Advances in Colloid and Interface Science* **2006**, *128-130*, 37–46.

(9) Schuettfort, T.; Nish, A.; Nicholas, R. J. *Nano letters* **2009**, *9*, 3871–6.

(10) Stranks, S. D.; Sprafke, J. K.; Anderson, H. L.; Nicholas, R. J. *ACS nano* **2011**, *5*, 2307–15.

(11) Clavé, G. et al. *submitted* **2012**,

(12) Yang, M.; Koutsos, V.; Zaiser, M. *The journal of physical chemistry. B* **2005**, *109*, 10009–14.

(13) Nish, A.; Hwang, J.-Y.; Doig, J.; Nicholas, R. J. *Nature nanotechnology* **2007**, *2*, 640–6.

(14) Zheng, M.; Jagota, A.; Semke, E. D.; Diner, B. a.; McLean, R. S.; Lustig, S. R.; Richardson, R. E.; Tassi, N. G. *Nature materials* **2003**, *2*, 338–42.

(15) Arnold, M. S.; Stupp, S. I.; Hersam, M. C. *Nano letters* **2005**, *5*, 713–8.

(16) Yang, R.; Tang, Z.; Yan, J.; Kang, H.; Kim, Y.; Zhu, Z.; Tan, W. *Analytical chemistry* **2008**, *80*, 7408–13.

(17) Ernst, F.; Heek, T.; Setaro, A.; Haag, R.; Reich, S. *Advanced Functional Materials* **2012**, 10.1002/adfm.201200784.

(18) Casey, J. P.; Bachilo, S. M.; Weisman, R. B. *Journal of Materials Chemistry* **2008**, *18*, 1510.

(19) Roquelet, C.; Garrot, D.; Lauret, J. S.; Voisin, C.; Alain-Rizzo, V.; Roussignol, P.; Delaire, J. a.; Deleporte, E. *Applied Physics Letters* **2010**, *97*, 141918.

(20) Roquelet, C.; Lauret, J.; Alain-Rizzo, V.; Voisin, C.; Fleurier, R.; Delarue, M.; Garrot, D.; Loiseau, A.; Roussignol, P.; Delaire, J.; Others, *ChemPhysChem* **2010**, *11*, 1667.

(21) Wang, R. K.; Chen, W.-C.; Campos, D. K.; Ziegler, K. J. *Journal of the American Chemical Society* **2008**, *130*, 16330–7.

(22) Kördel, C.; Setaro, A.; Bluemmel, P.; Popeney, C. S.; Reich, S.; Haag, R. *Nanoscale* **2012**, *4*, 3029.

(23) Wyszogrodzka, M.; Haag, R. *Chemistry (Weinheim an der Bergstrasse, Germany)* **2008**, *14*, 9202–14.

(24) Frey, H.; Haag, R. *Reviews in Molecular Biotechnology* **2002**, *90*, 257–267.

(25) Cheng, Q.; Debnath, S.; Gregan, E.; Byrne, H. J. *Society* **2008**, 20154–20158.

(26) Popeney, C. S.; Setaro, A.; Mutihac, R.-C.; Bluemmel, P.; Trappmann, B.; Vonneman, J.; Reich, S.; Haag, R. *ChemPhysChem* **2012**, *13*, 203 – 211.

(27) Backes, C.; Hauke, F.; Hirsch, A. *Advanced Materials* **2011**, *23*, 2588–601.

(28) Heek, T.; Fasting, C.; Rest, C.; Zhang, X.; Würthner, F.; Haag, R. *submitted* **2012**,

(29) Heek, T.; Fasting, C.; Rest, C.; Zhang, X.; Würthner, F.; Haag, R. *Chemical Communications* **2010**, *46*, 1884–6.

Supporting Information

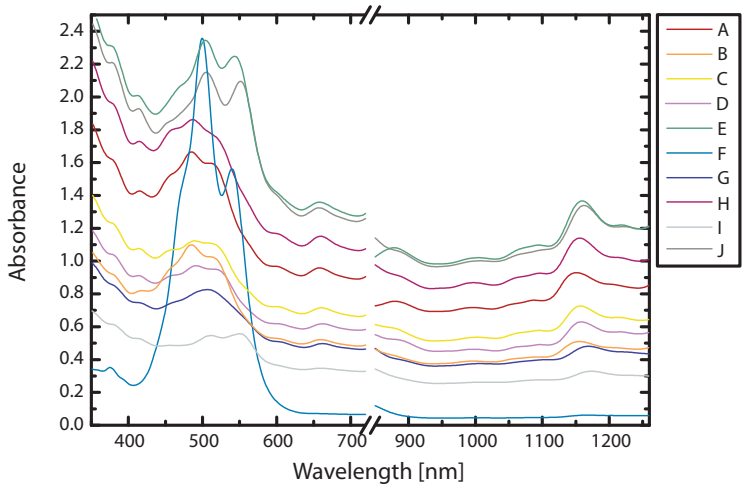

Figure 7: Absorbance measurements of HiPco nanotubes solubilized with compounds **A** - **H**. A chart of the chemical structures of all compounds can be found in Figure 1.

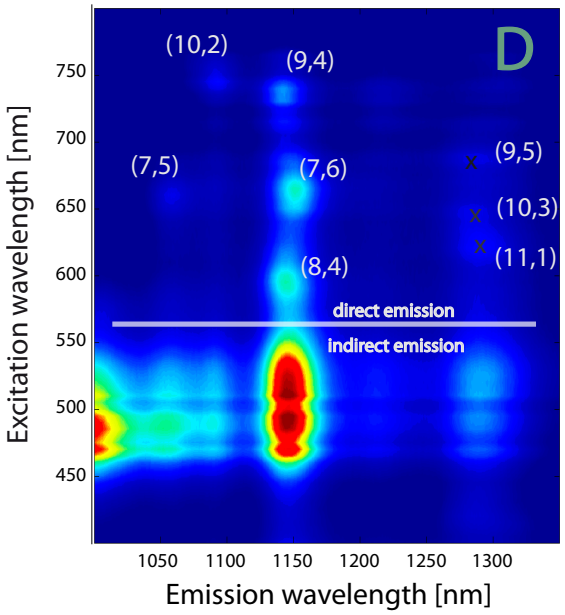

Figure 8: PLE map of nanotubes solubilized with compound **D**.

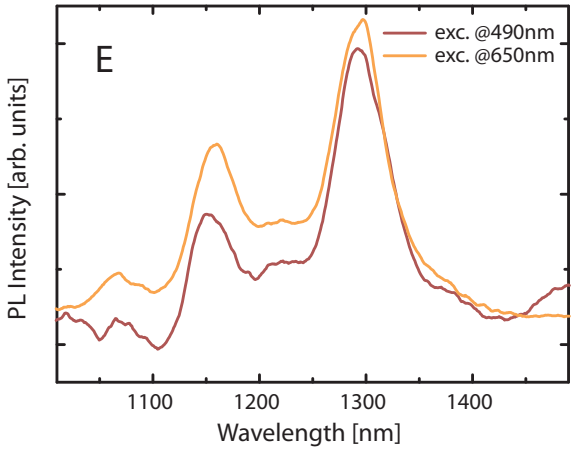

Figure 9: Photoluminescence lines at the direct and indirect excitation wavelengths of nanotubes solubilized with compound **E**.

Synthesis and Characterization of the Compounds

Materials

All solvents and reagents were purchased from commercial sources and used as received without further purification, unless otherwise stated. The solvents for spectroscopic studies were of spectroscopic grade and used as received. N-(2,6-Diisopropylphenyl)-perylene-3,4-monoimide was supplied by the BASF AG. Synthesis and characterization of compounds **I** ([G2]-PBI) and **B** ([G3]-PIDE-C10) have been recently reported by us.[28,29] The compounds **C** ([G3]-PIDE-C6) and **A** ([G3]-PIDE-C16) are prepared according to the synthetic protocol published for **B** ([G3]-PIDE-C10).[28] PG-dendrons[b 23] (H2N-[G3], H2N-[G3]-OH, HO-[G3]), mPEG1000-amine[c], 1-azido-6-bromohexane[d], perylene-3,4,9,10-tetracarboxylic-3,4-anhydride-9,10-imide[e], N-(1-hexyl- heptyl)-perylene-3,4,9,10-tetracarboxylic-3,4-anhydride-9,10-imide[f], 9,10-bis-(decyloxycarbonyl)-perylene-3,4,9,10-tetracarboxylic-3,4-anhydride[g] have been prepared according to literature.

General Methods

^{1}H NMR spectra were either recorded on a Jeol ECX 400 (400 MHz and 100 MHz for ^{1}H and ^{13}C, respectively) or a Delta Jeol Eclipse 700 spectrometer (700 MHz and 175 MHz for ^{1}H and ^{13}C, respectively) at 25°C and calibrated against residual solvent peaks as internal standard. NMR data was reported as follows: chemical shift, multiplicity (s=singlet, d=doublet, t=triplet, q=quartet), coupling constants(s) in Hertz (Hz) and integration. Multiplets (m) were reported over the range (ppm) at which they appear at the indicated field strength. IR spectra have been measured on a Nicolet Avatar 320 FT-IR. Elemental analyses were performed on a Perkin-Elmer EA 240. ESI-MS spectra were measured on an Agilent 6210 ESI-TOF, Agilent Technologies, Santa Clara, CA, USA. Solvent flow rate was adjusted to 10 μL/min, Spray voltage set to 4.000 V. Drying gas flow

[b] M. Wyszogrodzka, K. Möws, S. Kamlage, J. Wodzinska, B. Plietker, R. Haag, Eur. J. Org. Chem., 2008, 53 – 63.

[c] J.C. Neal, S. Stolnik, E. Schacht, E.R. Kenawy, M.C. Garnett, S.S. Davis, L. Illum, Pharm Sci 1998; 87: 1242-1248

[d] C. Romuald, E. Busseron, F. Coutrot, J. Org. Chem., 2010, 75, 6156

[e] H. Tröster, Dyes Pigm., 1984, 5, 171-177

[f] H. Kaiser, J. Lindner, H. Langhals, Chem. Ber., 1991, 124, 529-535

[g] C. Xue, R. Sun, R. Annab, D. Abadi, Tetrahedron Lett., 2009, 50, 853-856

rate was set up to 15 psi (1 bar). All other parameters were adjusted for a maximum abundance of the relative $[M+H]^+$. UV-Vis spectra were measured on a Perkin Elmer Lambda 950 spectrophotometer using 1 cm Quartz glass cuvettes. The steady state fluorescence spectra were measured on a Jasco FP-6500 fluorometer equipped with a Hamamatsu R928 Photomultiplier (corrected against photomultiplier and lamp intensity) using 1 cm quartz glass cuvettes. Ultrafiltration was performed in solvent-resistant stirred cells from Millipore (Billerica, MA) with Ultracel regenerated cellulose membranes (MWCO 1000 g mol^{-1} or MWCO 3000 g mol^{-1}).

Synthesis of C ([G3]-PIDE-C6) and A ([G3]-PIDE-C16)

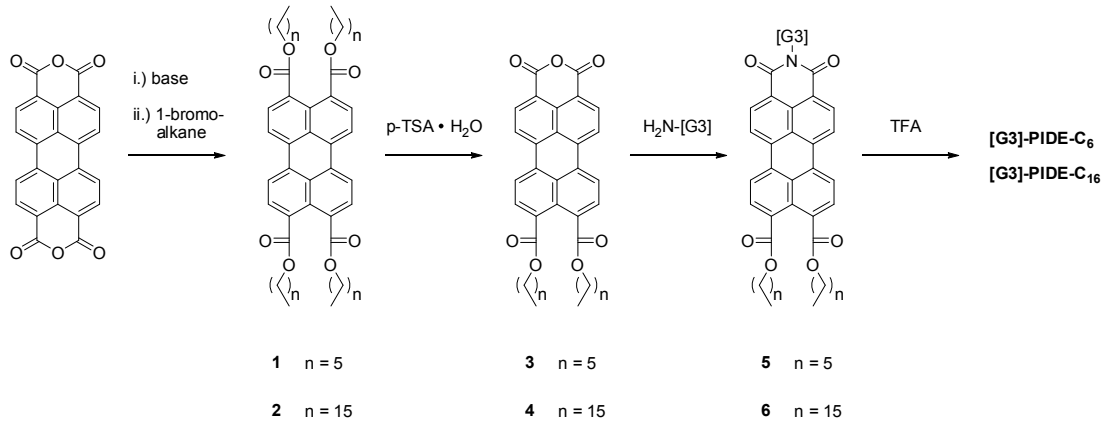

Figure 10: Synthesis scheme 1

Synthesis of 1: 3.92 g (10 mmol, 1 eq.) PBA have been suspended in 250 ml water and 6 g (150 mmol) NaOH were added. After being stirred overnight unsoluble material was filtered off and the pH was adjusted to 8 by adding HCl. Afterwards 0.3 g (1.8 mmol, 5.5 eq.) KI and 2.7 g (5 mmol) TOAB have been added and stirred for 20 minutes. Subsequently 11.2 ml (80 mmol) 1-bromohexane were added and the mixture was refluxed overnight. After being cooled to room temperature the crude mixture was diluted with chloroform, the organic layer separated, washed three times with water and dried over $MgSO_4$. Purification of the yellow orange crude product was achieved via column chromatography (silicagel, DCM) and subsequent recrystallization in EtOH.

The yield was 7.04 g (9 mmol, 92% yield) of **1** as a yellow powder. The analytical data matched the reported literature values.[h]

IR (ATR) 2952 (m), 2930 (m), 2891 (m), 2866 (m), 1727 (s), 1710 (s), 1589 (m), 1514 (w), 1478 (m), 1409 (m), 1390 (w), 1376 (w), 1331 (w), 1307 (m), 1264 (s), 1183 (s), 1160 (s), 1134 (s), 1066 (m), 999 (s), 935 (m), 842 (s), 805 (s), 772 (m), 746 (s). ^{1}H NMR ($CDCl_3$, 400 MHz): δ (ppm) = 8.29 (d, 8.0 Hz, 4H); 8.04 (d, 7.9 Hz, 4H); 4.32 (t, 6.9 Hz, 8H); 1.79 (q, 7.0 Hz, 8H); 1.51-1.22 (m, 24H); 0.91 (t, 7.0 Hz, 12H). UV/Vis ($CHCl_3$): λ_{max} (E_{rel}) 472 (1.00), 443 (0.81), 419 (0.40) nm. Fluorescence ($CHCl_3$): λ_{max} (E_{rel}) = 493 (1.00), 521 (0.70). Elemental Analysis calcd. for $C_{48}H_{60}O_8$, C 75.36 H 7.91 found C 74.98, H 7.96.

Synthesis of 2: Same procedure as for **1** with 24.5 ml of 1-bromohexadecane. The yield was 4.11 g (31% yield) of **2** as a yellow powder.

IR (ATR) 2954 (w), 2918 (s), 2849 (s), 1730 (s), 1718 (s), 1592 (m), 1472 (m), 1464 (m), 1412 (w), 1377 (m), 1311 (w), 1281 (s), 1171 (s), 1142 (s), 1095 (w), 1048 (w), 1022 (w), 1002 (w), 937 (w), 849 (m), 805 (m), 746 (s), 724 (m), 717 (m). ^{1}H NMR ($CDCl_3$, 400 MHz): δ (ppm) = 8.28 (d, 8.1 Hz, 4H); 8.04 (d, 7.9 Hz, 4H); 4.31 (t, 6.9 Hz, 8H); 1.78 (q, 7.0 Hz, 8H); 1.43 (q, 6.9 Hz, 8H); 1.37-1.17 (m, 96H); 0.86 (t, 7.0 Hz, 12H). UV/Vis ($CHCl_3$): λ_{max} (E_{rel}) 472 (1.00), 443 (0.81), 419 (0.40) nm. Fluorescence ($CHCl_3$): λ_{max} (E_{rel}) = 491 (1.00), 522 (0.66). Elemental Analysis calcd. for $C_{88}H_{140}O_8$, C 79.71 H 10.64 found C 78.98, H 10.67.

Synthesis of 3: 3 g (3.92 mmol, 1eq.) 1 were dissolved in 5 ml of a mixture of toluene and n-dodecane (1: 7) and heated to 95 ^{circ}C. Then 0.75 g (3.92 mmol, 1 eq.) pTSAxH_2O have been added and the mixture was stirred until no starting material was detectable anymore (1.5 h) and cooled to room temperature. The red solid was dissolved in Chloroform and purified via column chromatography (silicagel, Chloroform: Aceton 30:1) and recrystallized in EtOH giving 1.77 g (78 % yield) of **3** as a red solid.

IR (ATR) 2953 (m), 2929 (m), 2857 (m), 1764 (s), 1708 (s), 1592 (s), 1510 (m), 1456 (m), 1413 (m), 1380 (w), 1341 (m), 1324 (m), 1281 (s), 1254 (s), 1202 (m), 1148 (s), 1123 (s), 1104

[h] X. Mo, M.-M. Shi, J.-C. Huang, M. Wang, H.-Z. Chen, Dyes Pigm., 2008, 76, 236 – 242

(w), 1061 (m), 1010 (s), 908 (w), 858 (s), 841 (m), 805 (s), 750 (w), 737 (s), 691 (w). ^{1}H NMR ($CDCl_3$, 400 MHz): δ (ppm) = 8.60 (d, 7.6 Hz, 2H); 8.45 (m, 4H); 8.10 (d, 7.8 Hz, 2H); 4.34 (t, 6.8 Hz, 4H); 1.81 (q, 7.0 Hz, 4H); 1.47 (q, 7.7 Hz, 4H); 1.41-1.29 (m, 8H), 0.91 (t, 6.7 Hz, 6H). UV/Vis ($CHCl_3$): λ_{max} (E_{rel}) 506 (1.00), 477 (0.83), 448 (0.41) nm. Fluorescence ($CHCl_3$): λ_{max} (E_{rel}) = 532 (1.00), 567 (0.70). Elemental Analysis calcd. for $C_{36}H_{34}O_7$, C 74.72 H 5.92 found C 74.88, H 6.01.

Synthesis of 4: Same procedure as for **3** with 3 g (2.26 mmol, 1eq.) of **2**, 0.43 g (2.26 mmol, 1eq.) pTSAxH_2O and 5 ml of a mixture of toluene and n-dodecane (1: 4). Purification was done via column chromatography (silicagel, Chloroform: Aceton 18:1) The yield was 1.26 g (65 % yield) of **4** as a red powder.

IR (ATR) 2954 (w), 2918 (s), 2850 (s), 1766 (s), 1734 (s), 1708 (s), 1593 (s), 1511 (w), 1469 (m), 1415 (w), 1341 (w), 1328 (w), 1285 (s), 1251 (s), 1204 (w), 1151 (s), 1126 (s), 1097 (w), 1058 (w), 1010 (s), 857 (m), 841 (m), 806 (s) 752 (m), 736 (s), 722 (w), 690 (w). ^{1}H NMR ($CDCl_3$, 400 MHz): δ (ppm) = 8.62 (d, 8.0 Hz, 2H); 8.49 (d, 7.8 Hz, 2H); 8.47 (d, 7.8 Hz, 2H); 8.12 (d, 7.9 Hz, 2H); 4.33 (t, 6.9 Hz, 4H); 1.80 (q, 6.9 Hz, 4H); 1.43 (q, 7.2 Hz, 4H); 1.40-1.02 (m, 48H); 0.86 (t, 6.6 Hz, 6H). UV/Vis ($CHCl_3$): λ_{max} (E_{rel}) 506 (1.00), 477 (0.83), 448 (0.41) nm. Fluorescence ($CHCl_3$): λ_{max} (E_{rel}) = 532 (1.00), 567 (0.70). Elemental Analysis calcd. for $C_{56}H_{74}NO_7$, C 78.28 H 8.68 found C 78.98, H 8.79.

Synthesis of 5: 200 mg (0.14 mmol, 1.1 eq.) H2N-[G3], 73 mg (0.13 mmol, 1eq.) **3** and 200 mg imidazol were added to a 25 ml schlenk flask. The mixture was heated under argon for 4 h and cooled to room temperature. The crude product was dissolved in a small amount of DCM and purified via column chromatography (silica gel, EtOAc:Hexane:MeOH, 60:40:2). The product **5** was obtained as 227 mg (90% yield) of a red honey like oil.

IR (ATR) 2985 (m), 2924 (s), 2857 (s), 1718 (br s), 1698 (s), 1658 (s), 1594 (s), 1511 (w), 1456 (m), 1416 (m), 1370 (s), 1295 (s), 1258 (s), 1211 (s), 1154 (s), 1072 (s), 1052 (s), 975 (m), 843 (s), 809 (s), 749 (s), 700 (m). ^{1}H NMR (CD_2Cl_2, 700 MHz): δ (ppm) = 8.61 (br m, 2H); 8.54 (d, 7.9 Hz, 2H); 8. 51 (d, 8.0 Hz, 2H); 8.11 (d, 7.8 Hz, 2H); 5.58 (m, 1H), 4.3 (t, 6.9 Hz,

4H); 4.22 (m, 2H), 4.19 (m, 4H); 4.09 (m, 4H); 4.03 (m, 2H); 3.99 (m, 4H); 3.91 (m, 4H); 3.66 (m, 4H); 3.60-3.26 (m, 50H); 1.79 (t, 7.2 Hz, 4H); 1.45 (t, 7.2 Hz, 4H); 1.40-1.22 (m, 56H); 0.88 (t, 7.1 Hz, 6H). MS (ESI-TOF-HRMS, pos. mode) m/z = 2032.0473 $[M+Na]^+$ (calculated mass $[C_{105}H_{157}NO_{36}Na]^+$ 2032.0411). UV/vis (DCM): λ_{max} (E_{rel}) 504 (1.00), 473 (0.75), 444 (0.33) nm. Fluorescence (DCM): λ_{max} (E_{rel}) = 530 (1.00), 561 (0.78) nm. Elemental Analysis calcd. for $C_{105}H_{157}NO_{36}$, C 62.76, H 7.88, N 0.70 found C 62.52, 7.97, N 0.68.

Synthesis of 6: Same procedure as for **5** using 200 mg (0.14 mmol, 1.1 eq.) H2N-[G3], 108 mg (0.13 mmol, 1eq.) **4** and 200 mg imidazol. Purification was done via column chromatography (silica gel, EtOAc:Hexane:MeOH, 60:40:2). The yield was 267 mg (93% yield) of **6** as a red honey like oil.

IR (ATR) 2985 (m), 2923 (s), 2857 (s), 1718 (br s), 1698 (s), 1658 (s), 1594 (s), 1512 (w), 1456 (m), 1418 (m), 1370 (s), 1297 (s), 1258 (s), 1212 (s), 1154 (s), 1074 (s), 1052 (s), 975 (m), 843 (s), 808 (s), 747 (s), 699 (m). ^{1}H NMR (CD_2Cl_2, 700 MHz): δ (ppm) = 8.61 (br m, 2H); 8.54 (d, 7.9 Hz, 2H); 8. 51 (d, 8.0 Hz, 2H); 8.11 (d, 7.8 Hz, 2H); 5.58 (m, 1H), 4.3 (t, 6.9 Hz, 4H); 4.22 (m, 2H), 4.19 (m, 4H); 4.09 (m, 4H); 4.03 (m, 2H); 3.99 (m, 4H); 3.91 (m, 4H); 3.66 (m, 4H); 3.60-3.26 (m, 50H); 1.79 (t, 7.2 Hz, 4H); 1.45 (t, 7.2 Hz, 4H); 1.40-1.22 (m, 96H); 0.88 (t, 7.1 Hz, 6H). MS (ESI-TOF-HRMS, pos. mode) m/z = 2312.3607 $[M+Na]^+$ (calculated mass $[C_{125}H_{197}NO_{36}Na]$+ 2312.3542). UV/vis (DCM): λ_{max} (E_{rel}) 504 (1.00), 473 (0.75), 444 (0.33) nm. Fluorescence (DCM): λ_{max} (E_{rel}) = 530 (1.00), 561 (0.78) nm. Elemental Analysis calcd. for $C_{125}H_{197}NO_{36}$, C 65.56, H 8.67, N 0.61 found C 65.77, 8.78, N 0.60.

Synthesis of compound C ([G3]-PIDE-C6)

9,10–Bis(hexyloxycarbonyl)perylene–N–(methyl(1,1):{2-oxapropyl(3,3)}$^{G1,G2}_{2x,4x}$: {2-oxapentyl (5,4)}$^{G3}_{8x}$: hydroxy$_{16}$–cascadane)–3,4–dicarboximide, Figure 11.

Deprotection was done by dissolving 100 mg (0.05 mmol, 1 eq.) **5** in 5 ml of a mixture of DMSO and water (1:3) adding 0.1 ml TFA and heating to 50 °C over night. Afterwards 100 ml of water were added and the crude product was purified via ultrafiltration against water (MWCO 1000). A subsequent freezedrying gave 82 mg (98% yield) of the final product as a red fluffy solid.

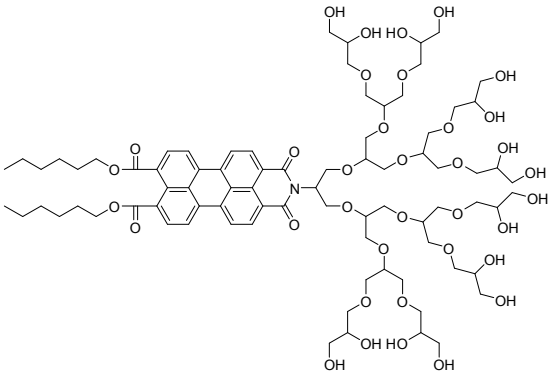

Figure 11: Chemical structure of compound **C**

IR (ATR) 3377 (br s), 2924 (s), 2872 (s), 1717 (m), 1695 (s), 1652 (m), 1593 (m), 1511 (w), 1457 (m), 1417 (m), 1358 (m), 1295 (m), 1262 (s), 1211 (w), 1082 (br s), 929 (m), 850 (m), 828 (w), 807 (m), 773 (w), 748 (s), 719 (w), 668 (w). ^{1}H NMR (CD_3OD, 700 MHz): δ (ppm) = 8.28-7.82 (br m, 8H); 5.73 (q, 6.6Hz, 1H); 4.46 (m, 6H); 4.26-4.19 (br m, 2H), 3.84-3.35 (m, 70H, PG-Dendron), 1.91 (q, 6.9Hz, 4H); 1.58 (q, 7,3Hz, 4H); 1.52-1.42 (m, 8H); 0.99 (t, 6.7Hz, 6H). MS (ESI-TOF-HRMS, pos. mode) m/z = 1710.8085 $[M+Na]^+$ (calculated mass $[C_{81}H_{125}NO_{36}Na]^+$ 1710.7874). UV/Vis (Dioxan): λ_{max} (E_{rel}) 504 (1.00), 473 (0.76) nm. Fluorescence (Dioxan): λ_{max} (E_{rel}) = 526 (1.00), 559 (0.73). Elemental Analysis calcd. for $C_{81}H_{125}NO_{36}$, C 57.61, H 7.46, N 0.83 found C 57.05, H 7.49, N 0.77.

Synthesis of compound A ([G3]-PIDE-C16)

9,10–Bis(hexadecyloxycarbonyl)perylene–N–(methyl(1,1):{2-oxapropyl(3,3)}$^{G1,G2}_{2x,4x}$: {2-oxapentyl (5,4)}$^{G3}_{8x}$: hydroxy$_{16}$–cascadane)–3,4–dicarboximide

Same procedure as for **C** using 100 mg (0.044 mmol, 1eq.) **6**. The yield was 82 mg (95% yield) of **6** as a red honey like oil. The characterization has been reported elsewhere.[17]

Synthesis of compound H (mPEG1k-PIDE-C10)

9,10–Bis(decyloxycarbonyl)perylene–N-(mPEG1000)–3,4–dicarboximide, Figure 12.

200 mg (0.2 mmol, 1.1 eq.) mPEG1000-amine, 126 mg (0.18 mmol, 1eq.) 9,10-bis-(decyloxycarbonyl)-perylene-3,4,9,10-tetracarboxylic–3,4–anhydride and 300 mg imidazol were added to a 25 ml

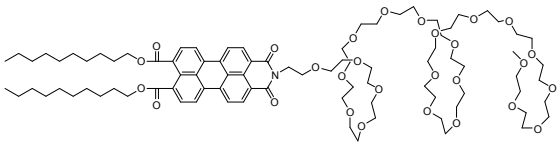

Figure 12: Chemical structure of compound **H**

schlenk flask. The mixture was heated under argon for 4 h and cooled to room temperature. The crude product was dissolved in a small amount of DCM and purified via column chromatography (silica gel, CHCl3:MeOH, 97:3). The product was obtained as 292 mg (97% yield) of a red wax.

IR (ATR) 2921 (m), 2883 (s), 2855 (w), 1717 (w), 1699 (s), 1652 (m), 1594 (m), 1511 (w), 1466 (m), 1417 (w), 1361 (m), 1343 (s), 1296 (m), 1268 (m), 1242 (m), 1217 (w), 1198 (w), 1146 (w), 1103 (br s), 962 (br s), 843 (s), 807 (m), 747 (s), 720 (w), 697 (w). ^{1}H NMR (CD_3OD, 700 MHz): δ (ppm) = 8.32 (d, 7.6 Hz, 2H); 8.11 (d, 7.2 Hz, 2H); 8.07 (d, 7.2 Hz, 2H); 7.94 (d, 7.6 Hz, 2H); 4.40 (t, 5.8 Hz, 2H); 4.33 (t, 6.8 Hz, 4H); 3.85 (t, 5.9 Hz, 2H); 3.73 (m, 2H); 3.66-3.54 (m, 74H, PEG backbone); 3.52 (m, 2H); 3.32 (s, 3H); 1.81 (q, 7.2 Hz, 4H); 1.45 (q, 7.2 Hz, 4H); 1.37 (q, 7.1 Hz, 4H); 1.35-1.23 (m, 20H); 0.85 (t, 6.9 Hz, 6H). MS (ESI-TOF-HRMS, pos. mode) m/z = 1695.9546 $[M+Na]^+$ (calculated mass $[C_{89}H_{141}NO_{28}Na]^+$ 1695.9566). UV/Vis (DMSO): λ_{max} (E_{rel}) 502 (1.00), 474 (0.82) nm. Fluorescence (DMSO): λ_{max} (E_{rel}) = 534 (1.00), 565 (0.81). Elemental Analysis calcd. for $C_{89}H_{141}NO_{28}$, C 63.89, H 8.49, N 0.84 found C 62.42, H 8.77, N 0.80.

Synthesis of compound G ([G3]-PMI)

Synthesis of 7 In a 100ml flask 1 g (2.1 mmol, 1 eq.) N-(2,6-Diisopropylphenyl)perylene-3,4-monoimide was suspended in 100 ml tert-butanol. The mixture was brought to reflux and 4.15 g (104 mmol. 50 eq.) of KOH were added. The colour changed from red to yellow/green. After refluxing for 4 h the mixture was cooled to room temperature. Then 100 ml of a 1:1 mixture of 1 N HCl : acetic acid were added. The formed precipitate was filtered with a G4 glass frit and washed until neutral. Afterwards the precipitate was suspended in 200 ml aqueous potassium carbonate

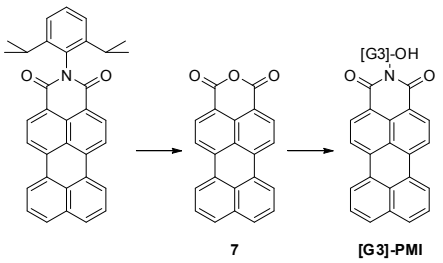

Figure 13: Synthesis scheme 2

solution (10% w/w) and brought to reflux. The resulting dark green solution was hot filtered to remove insoluble starting material. Subsequently the filtrate was acidified by the addition of concentrated HCl and refluxed for 20 minutes. The resulting precipitate was filtered and oven dried to give 0.4 g (59% yield) of **2** as of a brown-red powder. The analytical data matched literature values.[i] Elemental Analysis calcd. for $C_{22}H_{10}O_3$, C 81.98, H 3.31 found C 81.72, H 3.27.

Synthesis of compound G ([G3]-PMI)

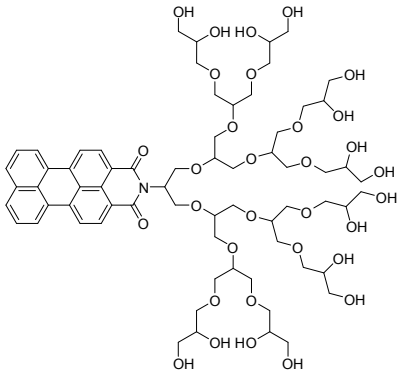

Figure 14: Chemical structure of compound **G**

N–(methyl(1,1):{2-oxapropyl(3,3)}$^{G1,G2}_{2x,4x}$: {2-oxapentyl(5,4)}$^{G3}_{8x}$: hydroxy$_{16}$–cascadane) –3,4–perylenedicarboximide, Figure 14.

In a 25 ml Schlenk-flask 100 mg (0.089 mmol, 1.1 eq) H2N-[G3]-OH, 26 mg (0.08 mmol, 1 eq.) **8** and 100 mg imidazol were added. The mixture was heated under argon at 140^{circ}C for 4h and

[i] K. Feiler, H. Langhals, K. Polborn, Liebigs Ann., 1995, 1229

cooled to room temperature. The crude product mixture was dissolved in water and filter through a 2 μm PTFE syringe filter. Purificaton was performed via RP-phase column chromatography (RP-18 silica gel, H2O:MeOH, 70:30). After evaporation of the solvent and a subsequent freezedrying 97 mg (85% yield) of [G3]-PMI were obtained as a red honey like oil.

IR (ATR) 3370 (br s), 2915 (s), 2872 (s), 1683 (s), 1643 (s), 1619 (s), 1591 (s), 1571 (s), 1457 (m), 1411 (w), 1357 (s), 1291 (m), 1247 (m), 1200 (w), 1039 (br s), 927 (m), 839 (w), 810 (s), 753 (s), 714 (w), 668 (w). ^{1}H NMR (CD_3OD, 700 MHz): δ (ppm) = 7.98-7.70 (br m, 4H); 7.70-7.54 (br m, 4H); 7.35-7.25 (br m, 2H); 5.61 (q, 6.3Hz, 1H); 4.45-4.28 (br m, 2H); 4.24-4.11 (br m, 2H), 3.84-3.34 (m, 70H, PG-Dendron). MS (ESI-TOF-HRMS, pos. mode) m/z = 1454.6246 $[M+Na]^+$ (calculated mass $[C_{67}H_{101}NO_{32}Na]^+$ 1454.6199). UV/Vis (DMSO): λ_{max} (E_{rel}) 504 (1.00), 488 (0.99) nm. Fluorescence (DMSO): λ_{max} (E_{rel}) = 564 (1.00), 601 (0.87). Elemental Analysis calcd. for $C_{67}H_{101}NO_{32}$, C 56.18, H 7.11, N 0.98 found C 55.98, H 7.16, N 0.87.

Synthesis of J ([G3]-hex-PBI) and D ([G3]-hex-PIDE-C6)

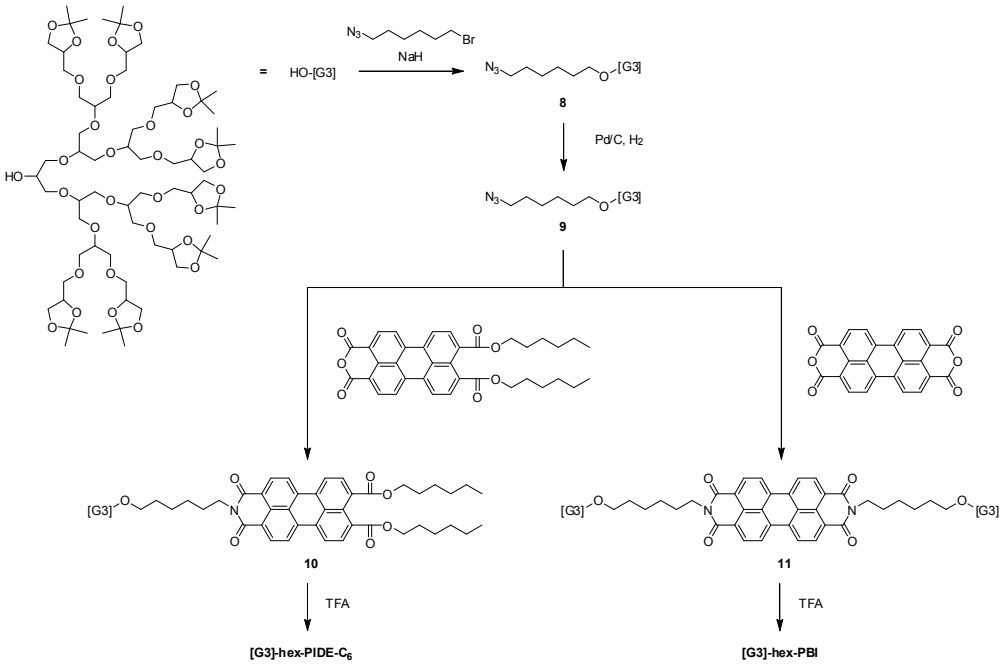

Figure 15: Synthesis scheme 3

Synthesis of 8 3 g (2.1 mmol, 1eq.) HO-[G3] were dissolved in 50 ml dry THF and 0.13 g

(3.15 mmol, 1.5 eq.) NaH (60% in mineral oil) were added. The mixture was stirred at 40°C for 3 h. Subsequently 0.65 g (3.15 mmol, 1.5 eq.) of 1-azido-6-bromohexane were added and the mixture was refluxed for 16 h. After cooling to room temperature THF was removed and the residue was dissolved in DCM and washed three times with water. The organic phase was dried over $MgSO_4$, filtered and the excess DCM was removed under vacuo. The remaining crude product was purified via column chromatography (silica gel, EtOAc:Hexane:MeOH, 60:40:3). The product **8** was obtained as 2.41 g (74% yield) of a colorless oil.

IR (ATR) 2986 (m), 2932 (s), 2875 (m), 2099 (m), 1456 (m), 1386 (w), 1376 (w), 1256 (s), 1214 (m), 1082 (m), 1066 (m), 975 (s), 920 (w), 844 (s), 792 (w), 772 (m), 746 (s). ^{1}H NMR (CD_2Cl_2, 400 MHz): δ (ppm) = 4.20 (m, 8H); 4.0 (m, 8H); 3.70-3.39 (m, 61H); 3.25 (t, 7.0 Hz, 2H); 1.59 (q, 7.0 Hz, 2H); 1.53 (q, 6.8 Hz, 2H); 1.39-1.20 (m, 52H). MS (ESI-TOF-HRMS, pos. mode) m/z = 1596.9011 $[M+Na]^+$ (calculated mass $[C_{75}H_{135}N_3O_{31}Na]^+$ 1596.8972). Elemental Analysis calcd. for $C_{75}H_{135}N_3O_{31}$, C 57.20, H 8.92, N 2.67 found C 56.96, H 8.82, N 2.61.

Synthesis of 9 2 g (1.3 mmol, 1eq.) **8** were dissolved in 150 ml MeOH in a high pressure reaction vessel and 0.14 g (0.13 mmol, 10 mol% Pd) Pd/C (10% w/w) added. The reaction vessel was sealed, Hydrogen (5 bar) was injected, and the mixture stirred for 24 h at room temperature. Then MeOH was removed in vacuo and the remaining residue purified via column chromatography (silica gel, EtOAc:Hexane:MeOH 60:40:15). The product **9** was obtained as 1.96 g (90% yield) of a slightly yellow oil.

IR (ATR) 2986 (m), 2932 (m), 2874 (m), 2866 (m), 1682 (m), 1456 (m), 1380 (w), 1371 (w), 1257 (s), 1214 (m), 1082 (m), 1054 (m), 975 (s), 920 (w), 844 (s), 805 (s), 792 (m), 746 (s). ^{1}H NMR (CD_2Cl_2, 400 MHz): δ (ppm) = 4.20 (m, 8H); 4.0 (m, 8H); 3.70-3.39 (m, 61H); 2.88 (t, 6.9 Hz, 2H); 1.61 (q, 7.1 Hz, 2H); 1.53 (q, 6.9 Hz, 2H); 1.39-1.20 (m, 52H). MS (ESI-TOF-HRMS, pos. mode) m/z = 1570.9103 $[M+Na]^+$ (calculated mass $[C_{75}H_{137}NO_{31}Na]^+$ 1570.9067). Elemental Analysis calcd. for $C_{75}H_{137}NO_{31}$, C 58.16, H 8.92, N 0.90 found C 57.99, H 8.97, N 0.87.

Synthesis of 10 100 mg (0.065 mmol, 1.05 eq.) **9**, 36 mg (0.061 mmol, 1eq.) 9,10-bis

(hexyloxycarbonyl)-perylene-3,4-bisanhydride **3** and 100 mg imidazol were added to a 25 ml schlenk flask. The mixture was heated under argon for 4 h and cooled to room temperature. The crude product was dissolved in a small amount of DCM and purified via column chromatography (silica gel, EtOAc:Hexane:MeOH, 60:40:2). The product **10** was obtained as 102 mg (79% yield) of a red honey like oil.

IR (ATR) 2987 (m), 2924 (s), 2857 (s), 1718 (br s), 1698 (s), 1658 (s), 1594 (s), 1511 (w), 1458 (m), 1416 (m), 1370 (s), 1295 (s), 1258 (s), 1211 (s), 1154 (s), 1080 (s), 1052 (s), 984 (m), 843 (s), 809 (s), 773 (m), 749 (s), 700 (m). ^{1}H NMR (CD_2Cl_2, 700 MHz): δ (ppm) = 8.51 (d, 7.9 Hz, 2H); 8.38 (m, 4H); 8.05 (d, 7.8 Hz, 2H); 4.32 (t, 6.9 Hz, 4H); 4.21 (m, 8H); 4.16 (m, 2H); 4.00 (m, 8H); 3.68 (m, 8H); -3.67-3.42 (m, 53H); 1.81 (q, 7.0 Hz, 4H); 1.75 (q, 7.5 Hz, 2H); 1.59 (q, 6.9 Hz, 2H); 1.51-1.41 (m, 8H); 1.41-1.36 (m, 32H); 1.32-1.31 (m, 24H); 0.92 (t, 7.1 Hz, 6H). MS (ESI-TOF-HRMS, pos. mode) m/z = 2132.1314 $[M+Na]^+$ (calculated mass $[C_{111}H_{169}NO_{37}Na]^+$ 2132.1299). UV/vis (DCM): λ_{max} (E_{rel}) 503 (1.00), 472 (0.75), 443 (0.33) nm. Fluorescence (DCM): λ_{max} (E_{rel}) = 530 (1.00), 561 (0.77) nm. Elemental Analysis calcd. for $C_{111}H_{169}NO_{37}$, C 63.20, H 8.07, N 0.66 found C 62.11, H 8.11, N 0.63.

Synthesis of 11 100 mg (0.065 mmol, 2.1 eq.) **9**, 12 mg (0.031 mmol, 1eq.) 3,4,9,10-perylene tetracarboxylic bisanhydride and 100 mg imidazol were added to a 25 ml schlenk flask. The mixture was heated under argon for 4 h and cooled to room temperature. The crude product was dissolved in a small amount of DCM and purified via column chromatography (silica gel, EtOAc:Hexane:MeOH, 60:40:2). The product **11** was obtained as 92 mg (88% yield) of a deep red honey like oil.

IR (ATR) 2984 (s), 2925 (s), 2869 (s), 1691 (s), 1656 (s), 1594 (s), 1577 (m), 1446 (m), 1436 (m), 1405 (m), 1370 (m), 1339 (s), 1251 (s), 1212 (s), 1075 (s), 1051 (s), 972 (m), 928 (w), 848 (s), 810 (s), 747 (m). ^{1}H NMR (CD_2Cl_2, 700 MHz): δ (ppm) = 8.65 (d, 8.0 Hz, 4H); 8.62 (d, 8.1 Hz, 4H); 4.21 (m, 16H); 4.18 (m, 4H); 4.00 (m, 16H); 3.68 (m, 16H); 3.67-2.42 (m, 106H); 1.75 (q, 7.3 Hz, 4H); 1.58 (q, 7.3 Hz, 4H); 1.49-1.41 (m, 8H); 1.36 (m, 48H); 1.31 (m, 48H). MS (ESI-TOF-HRMS, pos. mode) m/z = 1749.9189 $[M+2Na]^{2+}$ (calculated mass $[C_{174}H_{278}N_2O_{66}Na_2]^{2+}$

1749.9155). UV/vis (DCM): λ_{max} (E_{rel}) 522 (1.00), 487 (0.66), 457 (0.25), 427 (0.07) nm. Fluorescence (DCM): λ_{max} (E_{rel}) = 538 (1.00), 579 (0.59), 626 (0.14) nm. Elemental Analysis calcd. for $C_{174}H_{278}N_2O_{66}$, C 60.50, H 8.11, N 0.81 found C 60.32, H 8.15, N 0.79.

Synthesis of compound D ([G3]-hex-PIDE-C6)

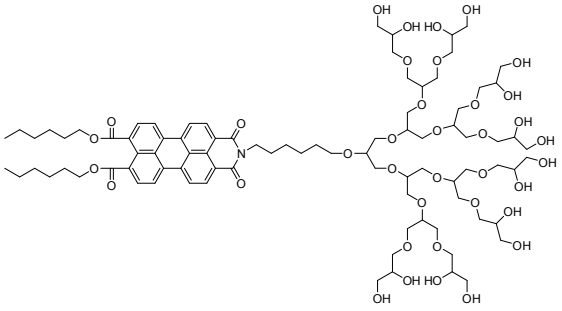

Figure 16: Chemical structure of compound **D**

9,10–Bis(hexyloxycarbonyl)perylene–N–(2-oxaoctyl(1,1):{2-oxapropyl(3,3)}$^{G1,G2}_{2x,4x}$: {2-oxapentyl (5,4)}$^{G3}_{8x}$: hydroxy$_{16}$–cascadane)–3,4–dicarboximide, Figure 16.

Deprotection was done by dissolving 70 mg (0.033 mmol, 1 eq.) **10** in 3 ml of a mixture of DMSO and water (1:3) adding 0.1 ml TFA and heating to 50°C over night. Afterwards 100 ml of water were added and the crude product was purified via ultrafiltration against water (MWCO 3000). A subsequent freezedrying gave 58 mg (98% yield) of the final product as a red fluffy solid.

IR (ATR) 3381 (br s), 2924 (s), 2870 (s), 1717 (m), 1694 (s), 1648 (s), 1594 (m), 1457 (m), 1417 (w), 1359 (m), 1296 (s), 1264 (s), 1201 (w), 1076 (br s), 931 (w), 849 (m), 806 (m), 747 (m), 668 (w). ^{1}H NMR (CD_3OD, 700 MHz): δ (ppm) = 7.95 (d, 7.6 Hz, 2H); 7.85 (d, 7.5 Hz, 2H); 7.76-7.70 (m, 4H); 4.36 (t, 6.9 Hz, 4H); 4.07 (t, 7.1 Hz, 2H); 3.80-3.45 (m, 81H); 1.89 (q, 7.1 Hz, 4H); 1.77 (q, 7.0 Hz, 4H); 1.67 (q, 6.9 Hz, 2H); 1.00 (t, 7.0 Hz, 6 H). MS (ESI-TOF-HRMS, pos. mode) m/z = 1810.8727 $[M+Na]^+$ (calculated mass $[C_{87}H_{137}NO_{37}Na]^+$ 1810.8762). UV/Vis (DMSO): λ_{max} (E_{rel}) 502 (1.00), 472 (0.8) nm. Fluorescence (DMSO): λ_{max} (E_{rel}) = 535 (1.00), 565 (0.83). Elemental Analysis calcd. for $[C_{87}H_{137}NO_{37}$, C 58.41, H 7.72, N 0.78 found C 57.88, H 7.63, N 0.73.

Synthesis of compound J ([G3]-hex-PBI)

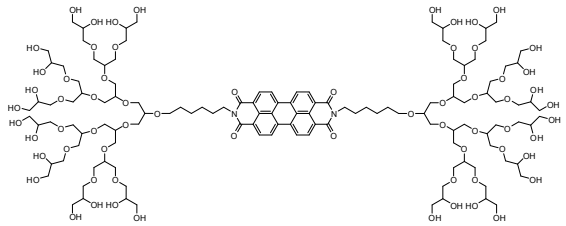

Figure 17: Chemical structure of compound **J**

N,N'–(2-oxaoctyl(1,1):{2-oxapropyl(3,3)}$^{G1,G2}_{2x,4x}$: {2-oxapentyl(5,4)}$^{G3}_{8x}$: hydroxy$_{16}$–cascadane) –3,4,9,10–perylenebis(dicarboximide), Figure 17.

Deprotection was done by dissolving 50 mg (0.014 mmol, 1 eq.) **11** in 3 ml of a mixture of DMSO and water (1:3) adding 0.1 ml TFA and heating to 50°C over night. Afterwards 100 ml of water were added and the crude product was purified via ultrafiltration against water (MWCO 3000). A subsequent freezedrying gave 20 mg (99% yield) of the final product as a red fluffy solid.

IR (ATR) 3371 (br s), 2919 (s), 2870 (s), 1691 (s), 1654 (s), 1594 (m), 1577 (w), 1442 (m), 1402 (m), 1384 (w), 1345 (s), 1250 (m), 1066 (s), 1039 (s), 928 (m), 856 (m), 809 (m), 746 (m), 658 (m). ^{1}H NMR (CD_3OD, 700 MHz): δ (ppm) = 8.05-7.70 (br m, 8H); 4.10-4.00 (br m, 4H); 3.82-3.47 (m, 154H, PG-Dendron& -CH_2-O-); 1.78 (m, 4H); 1.69 (q, 6.3 Hz, 4H); 1.54 (m, 8H). MS (ESI-TOF-HRMS, pos. mode) m/z = 1429.1582 $[M+2Na]^{2+}$ (calculated mass $[C_{126}H_{214}N_2O_{66}Na]^{2+}$ 1429.1635). UV/Vis (DMSO): λ_{max} (E_{rel}) 526 (1.00), 492 (0.70), 455 (0.27) nm. Fluorescence (DMSO): λ_{max} (E_{rel}) = 544 (1.00), 584 (0.66), 637 (0.17). Elemental Analysis calcd. for $C_{126}H_{214}N_2O_{66}$, C 53.80, H 7.67, N 1.00 found C 53.36, H 7.48, N 0.91.

Synthesis of compound E ([G3]-PBI-C13S)

Synthesis of 12 200 mg (0.14 mmol, 1.1 eq.) H_2N-[G3], 73 mg (0.13 mmol, 1eq.) N-(1-hexyl-heptyl)-perylene-3,4,9,10-tetracarboxylic-3,4-anhydride-9,10-imide and 200 mg imidazol were added to a 25 ml schlenk flask. The mixture was heated under argon for 4 h and cooled to room temperature. The crude product was dissolved in a small amount of DCM and purified via column chromatography (silica gel, EtOAc:Hexane:MeOH, 60:40:2). The product **12** was obtained as 194 mg (77% yield) of a deep red honey like oil.

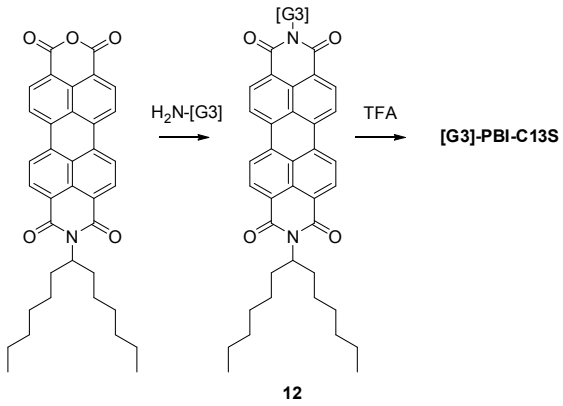

Figure 18: Synthesis scheme 4

IR (ATR) 2984 (s), 2925 (s), 2869 (s), 1696 (s), 1656 (s), 1594 (s), 1577 (m), 1456 (m), 1436 (m), 1405 (m), 1370 (m), 1339 (s), 1251 (s), 1212 (s), 1075 (s), 1051 (s), 972 (m), 918 (w), 842 (s), 810 (s), 747 (m). ^{1}H NMR (CD_2Cl_2, 400 MHz): δ (ppm) = 8.68-8.56 (br m, 8H); 5.58 (m, 1H); 5.17 (m, 1H); 4.23 (m, 2H); 4.18 (m, 4H); 4.08 (m, 6H); 3.99 (m, 4H); 3.91 (m, 4H); 3.66 (m, 4H); 3.61-3.21 (m, 50H); 2.24 (m, 2H); 1.84 (m, 2H); 1.38-1.20 (m, 64H); 0.83 (t, 6.9 Hz, 6H). MS (ESI-TOF-HRMS, pos. mode) m/z = 2027.0657 $[M+Na]^+$ (calculated mass $[C_{106}H_{158}N_2O_{34}Na]^+$ 2027.0622). Elemental Analysis calcd. for $C_{106}H_{158}N_2O_{34}$, C 63.52, H 7.95, N 1.40 found C 63.61, H 7.99, N 1.38. UV/vis (DCM): λ_{max} (E_{rel}) 522 (1.00), 487 (0.65), 457 (0.25), 426 (0.07) nm. Fluorescence (DCM): λ_{max} (E_{rel}) = 538 (1.00), 579 (0.59), 626 (0.14) nm. Elemental Analysis calcd. for $C_{106}H_{158}N_2O_{34}$, C 63.52, H 7.95, N 1.40 found C 63.12, 8.03, N 1.38.

Synthesis of compound E ([G3]-PBI-C13S)

N-(1-hexylheptyl)-N'–(methyl(1,1):{2-oxapropyl(3,3)}$^{G1,G2}_{2x,4x}$: {2-oxapentyl(5,4)}$^{G3}_{8x}$: hydroxy$_{16}$ –cascadane)–3,4,9,10–perylenebis(dicarboximide), Figure 19.

Deprotection was done by dissolving 150 mg (0.075 mmol, 1 eq.) **12** in 4 ml of a mixture of DMSO and water (1:3) adding 0.1 ml TFA and heating to 50°C over night. Afterwards 100 ml of water were added and the crude product was purified via ultrafiltration against water (MWCO 3000). A subsequent freezedrying gave 121 mg (99% yield) of the final product as a red fluffy

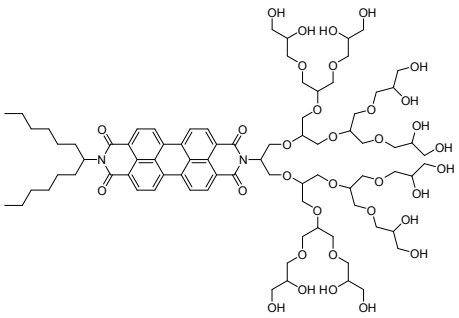

Figure 19: Chemical structure of compound **E**

solid.

IR (ATR) 3374 (br s), 2924 (s), 2870 (s), 1695 (s), 1655 (s), 1593 (s), 1576 (s), 1457 (m), 1435 (m), 1403 (m), 1339 (s), 1250 (m), 1213 (m), 1177 (w), 1042 (br s), 931 (w), 853 (m), 809 (s), 746 (s), 668 (m). ^{1}H NMR (CD_3OD, 700 MHz): δ (ppm) = 8.40-7.72 (br m, 8H); 5.55 (q, 6.1 Hz, 1H); 5.16 (m, 1H); 4.39-4.29 (br m, 2H); 4.28-4.16 (br m, 2H); 3.88-3.30 (m, 70 H, PG-Dendron); 2.33 (m, 2H); 1.96 (m, 2H); 1.55-1.30 (m, 16H); 0.91 (t, 7.1 Hz, 6H). MS (ESI-TOF-HRMS, pos. mode) m/z = 1705.8083 $[M+Na]^+$ (calculated mass $[C_{82}H_{126}N_2O_{34}Na]^+$ 1705.8084). UV/Vis (DMSO): λ_{max} (E_{rel}) 527 (1.00), 495 (0.82), 455 (0.34) nm. Fluorescence (DMSO): λ_{max} (E_{rel}) = 543 (1.00), 584 (0.68), 634 (0.20). Elemental Analysis calcd. for $C_{82}H_{126}N_2O_{34}$, C 58.49, H 7.54, N 1.66 found C 58.10, H 7.65, N 1.62.

Synthesis of compound F ([G3]-PBI-C10)

Synthesis of 13 200 mg (0.14 mmol, 1.1 eq.) H_2N-[G3], 49 mg (0.13 mmol, 1 eq.) perylene-3,4,9,10-tetracarboxylic-3,4-anhydride-9,10-imide and 400 mg imidazol were added to a 25 ml schlenk flask. The mixture was heated under argon for 4 h and cooled to room temperature. The crude product was dissolved in a small amount of DCM and purified via column chromatography (silica gel, EtOAc:Hexane:MeOH, 60:40:2). The product **13** was obtained as 197 mg (86% yield) of a deep red honey like oil.

IR (ATR) 3082 (w), 2984 (s), 2932 (s), 2872 (s), 1697 (s), 1660 (s), 1593 (s), 1577 (m), 1455 (m), 1433 (m), 1402 (m), 1369 (s), 1343 (s), 1255 (s), 1211 (s), 1073 (s), 1049 (s), 973 (m), 962 (w), 918(w), 840 (s), 810 (s), 793 (m), 741 (m). H NMR (CD_2Cl_2, 700 MHz): δ (ppm)

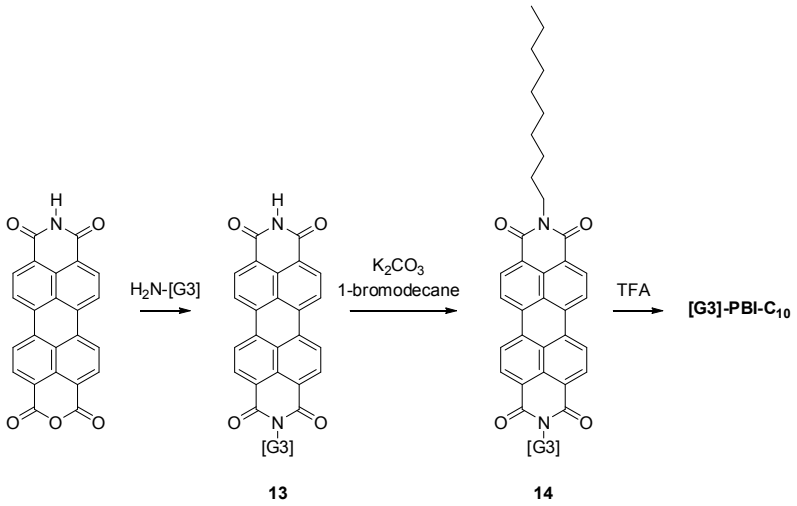

Figure 20: Synthesis scheme 5

= 9.65 (s, 1H); 8.49-8.17 (m, 8H), 5.62 (m, 1H), 4.41-3.38 (m, 74H), 1.36-1.23 (m, 48H). MS (ESI-TOF-HRMS, pos. mode) m/z = 1844.8599 $[M+Na]^+$ (calculated mass $[C_{93}H_{132}N_2O_{34}Na]^+$ 1844.8587). UV/vis (DCM): λ_{max} (E_{rel}) 522 (1.00), 487 (0.65), 457 (0.25), 426 (0.07) nm. Fluorescence (DCM): λ_{max} (E_{rel}) = 538 (1.00), 579 (0.59), 626 (0.14) nm. Elemental Analysis calcd. for $C_{93}H_{132}N_2O_{34}$, C 61.30, H 7.30, N 1.54 found C 61.13, H 7.28, N 1.55.

Synthesis of 14 150 mg (0.082 mmol, 1 eq.) **13** were dissolved in 2 ml dry DMF under argon atmosphere. Afterwards 341 mg (2.4 mmol, 30 eq.) potassium carbonate and 0.1 ml (0.412 mmol, 5 eq.) 1-bromodecane were added and the mixture was heated at 120°C for 18 h. After cooling to room temperature excess DMF was removed in vacuo and the crude product purified via column chromatography (silica gel, EtOAc:Hexane:MeOH, 60:40:2). The product **14** was obtained as 138 mg (86% yield) of a deep red honey like oil.

IR (ATR) 2985 (s), 2925 (s), 2869 (s), 1696 (s), 1656 (s), 1594 (s), 1577 (m), 1456 (m), 1436 (m), 1407 (m), 1372 (m), 1339 (s), 1254 (s), 1212 (s), 1075 (s), 1052 (s), 974 (m), 918 (w), 842 (s), 810 (s), 747 (m). ^{1}H NMR (CD_2Cl_2 , 400 MHz): δ (ppm) = 8.69-8.58 (br m, 8H); 5.58 (m, 1H), 4.23 (m, 2H); 4.18 (m, 6H); 4.08 (m, 6H); 3.99 (m, 4H); 3.92 (m, 4H); 3.67 (m, 4H); 3.62-3.19 (m, 50H); 1.74 (q, 7.3 Hz, 2H); 1.44 (q, 7.4 Hz, 2H); 1.40-1.21 (m, 60H);

0.91 (t, 7.0 Hz, 3H). MS (ESI-TOF-HRMS, pos. mode) m/z = 1985.0202 $[M+Na]^+$ (calculated mass $[C_{103}H_{152}N_2O_{34}Na]+$ 1985.0153). UV/vis (DCM): λ_{max} (E_{rel}) 522 (1.00), 487 (0.66), 457 (0.25), 427 (0.07) nm. Fluorescence (DCM): λ_{max} (E_{rel}) = 538 (1.00), 579 (0.59), 626 (0.14) nm. Elemental Analysis calcd. for $C_{103}H_{152}N_2O_{34}$, C 63.04, H 7.81, N 1.43 found C 62.67, H 7.87, N 1.40.

Synthesis of compound F ([G3]-PBI-C10)

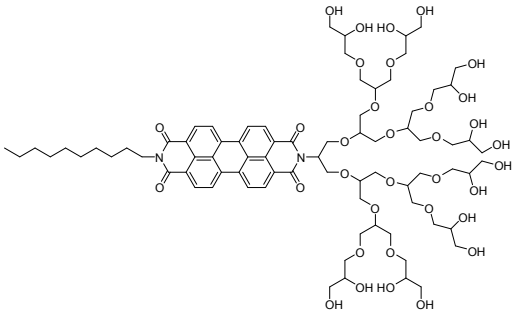

Figure 21: Chemical structure of compound **F**

N-(decyl)-N'–(methyl(1,1):{2-oxapropyl(3,3)}$^{G1,G2}_{2x,4x}$: {2-oxapentyl(5,4)}$^{G3}_{8x}$: hydroxy$_{16}$–cascadane)–3,4,9,10–perylenebis(dicarboximide), Figure 21.

Deprotection was done by dissolving 100 mg (0.051 mmol, 1 eq.) **14** in 3 ml of a mixture of DMSO and water (1:3) adding 0.1 ml TFA and heating to 50°C over night. Afterwards 100 ml of water were added and the crude product was purified via ultrafiltration against water (MWCO 3000). A subsequent freezedrying gave 80 mg (96% yield) of the final product as a red fluffy solid.

IR (ATR) 3347 (br s), 2922 (s), 2874 (s), 1693 (s), 1653 (s), 1594 (s), 1577 (m), 1457 (m), 1438 (m), 1403 (m), 1342 (s), 1253 (m), 1201 (m), 1180 (m), 1043 (br s), 929 (m), 854 (m), 810 (s), 746 (m), 720 (w), 668 (m). ^{1}H NMR (CD_3OD, 700 MHz): δ (ppm) = 8.30-7.61 (br m, 8H); 5.55 (br m, 1H); 4.41-4.32 (br m, 2H); 4.31-4.24 (br m, 2H), 4.30-3.92 (br m, 2H); 3.92-3.36 (m, 70H, PG-Dendron); 1.80-1.65 (br m, 2H); 1.55-1.28 (m, 14H); 0.93 (t, 6.1 Hz, 3H). MS (ESI-TOF-HRMS, pos. mode) m/z = 1663.7797 $[M+Na]^+$ (calculated mass $[C_{79}H_{120}N_2O_{34}Na]^+$ 1663.7615). UV/Vis (DMSO): λ_{max} (E_{rel}) 527 (1.00), 493 (0.71), 455 (0.31) nm. Fluorescence (DMSO):λ_{max} (E_{rel}) = 543 (1.00), 584 (0.63), 629 (0.17). Elemental Analysis

calcd. for $C_{79}H_{120}N_2O_{34}$, C 57.79, H 7.37, N 1.71 found C 57.13, H 7.21, N 1.65.